Photocatalytic degradation of potassium permanganate using zinc oxide nanoparticles

S. A. Al-Ghamdi[a,*], M. Rashad[a,b], Mohammed S. Al-Qarni[a], Fahad A. Al-Shehri[a],
Ahmed H. Mbarki[a], Mohammed A. Al-Rashidi[a], A. M. Abd-Elnaiem[b]
[a]Nanotechnology Research Laboratory, Department of Physics, Faculty of
Science, University of Tabuk, Tabuk P.O. Box 741, Tabuk 71491, Saudi Arabia
[b]Physics Department, Faculty of Science, Assiut University, Assiut 71516, Egypt

In this work, zinc oxide (ZnO) nanoparticles were prepared by the solid-solid reaction technique. The photocatalytic efficiency, using a ZnO nanoparticle as a catalyst, has been shown by investigating the degradation rate of an extreme quantity of potassium permanganate ($KMnO_4$) in wastewater. The $KMnO_4$ dye reveals a degradation rate of 47% by the irradiation of UV compared to less than 5% for methylene blue using the same experiment conditions by ZnO nanoparticles as a catalyst. Also, various kinetics models such as the pseudo-first-order, the pseudo-second-order, and the intra-particle diffusion models are applied to investigate the photocatalytic process. Moreover, Boyd and Elovic models were applied to study in detail the mechanisms of the photocatalytic degradation process.

1. Introduction

Metal oxide-based semiconductors receive much attention due to their promising properties, and hence various technological applications [1, 2]. Usually, metal oxides semiconductors are used for manufacturing the microelectronic apparatus, piezoelectric devices, numerous bio-, and chemical sensors, water purification, catalysts, *etc.* [3, 4]. Transition metal oxides cover a broad number of compounds, therefore their physical and chemical properties including practically all sections in material science. Besides, such oxides have unique properties that make them attractive to applications in electronics [5]. These unique properties resulted from the existence of vacancies, stacking faults, dislocations, and grain boundaries in such oxides. Due to the controllable optical bandgap in the transition metal oxides, can be applied as a photocatalyst, as they are used in specific reduction, particular oxidation, and dehydrogenation [6]. Other parameters could affect the photocatalytic process such as the surface structure of a substance, substrate concentration, and the presence of oxidants. Therefore, control the size as well as the shape of photocatalytic materials such as Al_2O_3, Fe_2O_3, ZrO_2, ZnO, and CuO, etc., could improve the photocatalytic activity [7, 8, 9, 10, 11, 12].

The number of surface and interface atoms can be enhanced by diminishing or reducing the particle size, creating stress/strain and associative structural perturbations [13]. The optoelectronic and mechanical parameters of nanoparticles can be controlled by adjusting the lattice strain. Additionally, various kinds of strains such as the intrinsic and extrinsic types are associated with the preparation method, annealing, and calcination processes [14]. Moreover, the interactions between substrate and nanoparticles affect such structural perturbations [15]. The metal oxides, such as ZnO and MgO nanoparticles, are characterized by promising properties and hence advanced physicochemical technology applications. Therefore the researchers are particularly focusing on the synthesis, characterization, and applications of the nanostructures of these materials [16]. Photocatalysts that are activated by UV irradiation could be applied for oxidizing the organic pollutants into nontoxic products and disinfecting certain bacteria. Amongst

---

* Corresponding author: saalghamdi@ut.edu.sa

many semiconductor metal oxides, ZnO has been widely studied concerning the photocatalytic degradation of various organic wastes. ZnO shows diverse types of morphology (such as nanorods, nanosheets, nanoflower, etc.), wide direct bandgap (~3.37 eV), and is easily prepared by various and simple methods (such as sol-gel, electrochemical deposition, hydrothermal, etc.). It has been published that the variation of the morphology of ZnO reveals different efficiencies of photocatalytic activity. For example, Gupta et al. investigated the photodegradation of MB for various shapes of ZnO nanostructures [17]. Similarly, Ma et al., and Zhai et al. have investigated the photocatalytic efficiency through the degradation of methyl orange (MO) using various morphologies of ZnO such as nano-rod arrays and nano-disks [18, 19]. Also, Zheng et al. have studied the photocatalytic efficiency during the degradation of MO using octahedron and rod-like porous ZnO nanocomposites under UV irradiation [20]. Moreover, it was observed the catalytic efficiency of porous ZnO octahedron is higher for samples calcined at 500 °C, compared to those calcined at 700 °C and the increase is attributed to the higher surface area [20]. It is well known, $KMnO_4$ dye is one of the strongest oxidizing agents through water treatment. Besides, when a human is dealt with a large amount of $KMnO_4$ dye, his tissue could react with the $KMnO_4$ dye [21]. Li et al. [22] explained the $KMnO_4$ dye reduction to MnO_2 via the waste iron oxide (*i.e.* BT-3) catalyst to the accumulation on its surface to produce Fe-Mn oxide. Their catalytic study reveals a good convincement with the pseudo-first-order model. Verma et al. [21] deduced the ability of the activated charcoal to retain $KMnO_4$ ions via the adsorption in the solution and applied the Langmuir and Freundlich isotherms to fit their data.

Up to date, many studies have been performed about the gainful parts of nanoparticles on water purification after using the oxidizing agents in an extreme quantity such as $KMnO_4$ dye [20-21]. To continue and expand the previous studies, in the present work, the preparation and growth of ZnO nanoparticles by the solid-solid reaction method have been investigated. Then, wasted water that has been polluted by a large quantity of $KMnO_4$ dye was eliminated by UV light with the assist of ZnO nanoparticles as a catalyst. Besides, the photocatalytic efficiency for the purification of polluted water by $KMnO_4$ dye was evaluated and various models were examined.

2. Experimental details

All the used chemicals in the present study are purchased from Sigma Aldrich Company and used without any further purifications. ZnO nanoparticles are prepared by the solid-solid reaction method under ambient conditions. For this purpose, 0.2 M $ZnCl_2.2H_2O$ has been added to 0.5 M NaOH in a crucible. The bluish color of the mixed solutions is gradually transformed to white color after vigorous string for 5-10 minutes at room temperature (RT). The appearance of this white color reveals the formation of ZnO nanoparticles. Then, the product was carefully filtered and washed using deionized water and then dried at 100 °C in a furnace wave for ¼ h.

The photocatalytic degradation process of ZnO nanoparticles was performed using the $KMnO_4$ dye as a waste material, and ZnO nanoparticles as a catalyst. In these experiments, ~0.02 mg of the ZnO was added to ~4 mL of $KMnO_4$ dye with a concentration of 8 mg/L. To ensure the dispersion of ZnO inside the $KMnO_4$ dye, the mixture was put in an ultrasonic for 10 minutes, then the mixture was moved to glass tubes under the UV lamp (6 Watt) and tubes are separated from the UV lamp by 15 cm. The absorbance of the $KMnO_4$ dye in the presence of the ZnO nanoparticles catalysis was measured for various irradiation times reaches 3 h. The UV-visible spectrophotometer model Jenway, 6300 was utilized to measure the absorbance at the wavelength range of 200 to 1100 nm at RT.

3. Results and discussions

The structural properties of the produced ZnO nanoparticles are extensively studied in our previous work [12]. In the present study, we have extended our previous work with some focus on the influence of UV irradiation time on the photocatalytic degradation of $KMnO_4$ dye assisted by the prepared ZnO nanoparticles as a catalyst. The samples of ZnO were prepared 1 year ago before

the photocatalytic tests, and the samples were kept at RT in the dark to ensure the adsorption equilibrium of ZnO. Photocatalytic degradation is one of the important objectives for scientists due to its ability for eliminating organic and inorganic wastes from the wasted water. Nanostructured and nanomorphology of metal oxides are received much interest nowadays as they present a promising class of materials that can be used as catalysts in the photocatalytic degradation process [23, 24].

As mentioned above, the main objective of this study is to use a semiconductor-based metal oxide such as ZnO nanoparticles to remove the extreme quantity of wastes such as $KMnO_4$ dye from the wasted water via the photocatalytic process. The absorption spectra of $KMnO_4$ dye using ZnO nanoparticles as a catalyst at various UV irradiation times (up to 3 h) are shown in Fig. 1. Generally observed in the absorbance of the $KMnO_4$ the presence of two distinct peaks located at λ equals 524 and 545 nm which are characterizing the absorbance in $KMnO_4$ solutions. Besides, it can be seen that $KMnO_4$ absorption reduces with the increasing duration of UV irradiation. The observed reduction in the absorbance with the UV irradiation duration confirms the assistant of ZnO nanoparticles as a catalyst for degrading the $KMnO_4$ dye.

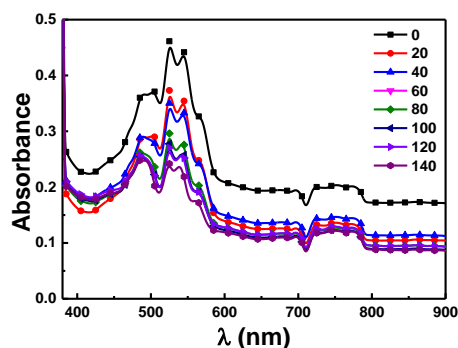*Fig. 1. Absorbance as a function of wavelength (λ) of $KMnO_4$ with ZnO nanoparticles as a catalyst.*

The photocatalytic degradation or the removal efficiency (η) of $KMnO_4$ debasement, is similar to other materials such as MB, MO, etc., can be evaluated from the following equation [25]:

$$\eta \ (\%) = \frac{C_o - C_t}{C_o} \times 100 = \frac{A_o - A_t}{A_o} \times 100 \qquad (1)$$

, where C_o is the initial concentration of waste, C_t is the residual concentration of waste after a fixed time (t), A_o is the initial absorbance of waste, with the absorbance of waste after a fixed time as A_t. As illustrated in Fig. 2a, the estimated value of η was significantly increased up to 37.6% as the UV irradiation time increased to 1 h, meanwhile, (η) slightly increased for a further increase in the UV irradiation time. Besides, $KMnO_4$ dye shows a degradation of 47% after 3 h of the UV irradiation assisted by ZnO nanoparticles as a catalyst compared to less than 5% for the degradation of MB (Fig. 2b) using the same ZnO catalyst at the same experimental conditions. As a comparison of the efficiency of ZnO nanoparticles measured by our previous work (17%) [12], it is concluded that natural aging plays an important factor in varying the efficiency of ZnO nanoparticles. It was noticed that the behavior is not a clear increase towards MB using ZnO nanoparticles. From this, we have concluded that experimentally ZnO could not use as catalysis for MB. Therefore, the work is going further for the degradation of $KMnO_4$ dye in the presence of ZnO nanoparticles.
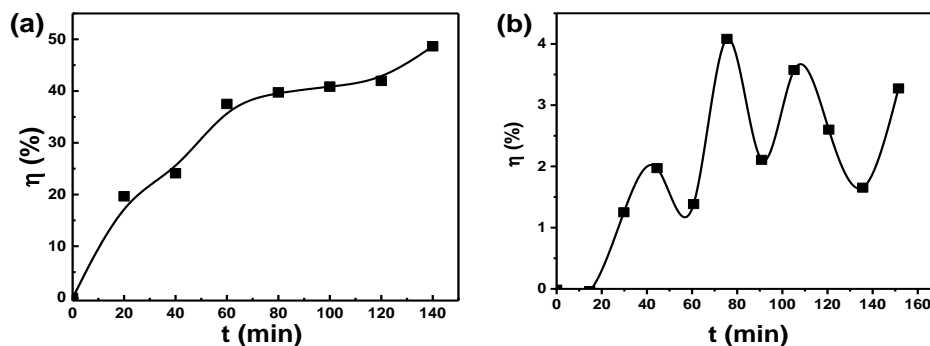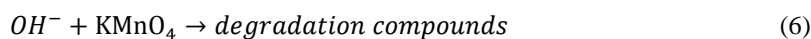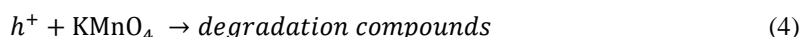
*Fig. 2. The photocatalytic efficiency (η) at various irradiation times (t) of (a) KMnO₄ debasement
and (b) methylene blue using ZnO nanoparticles.*

The photocatalytic mechanism is mainly defined as an electron-hole pair generation while a semiconductor sample is irradiated and able to undergo secondary reactions. As a catalyst is irradiated by UV radiation it receives a higher amount of energy than its bandgap and therefore the electron transits are forwarded from the valence band to the conduction band, leaving a hole in the valance band. The existence of such holes in the valence band could be the source of the oxidizing hydroxyl radicals. Accordingly, the holes can react with the dye and dynamic electrons therefore the degradation process takes place [26].

The photocatalytic degradation process using ZnO as a catalyst can be illustrated through three steps:

(i) The UV light falls on ZnO nanoparticles, then starts to degrade due to the formation of an electron (e^-) and hole (h^+) couples.

(ii) Thereafter a reaction between (h^+); $KMnO_4$ dye, and water takes place to generate OH^- radicals.

(iii) Finally, the reduction of oxygen adsorbed on the catalyst happens by the assistant of the (e^-) as a reductive agent [27, 28].

The mentioned above process can be introduced by the following equations:

$$Catalst\ (ZnO) + hv \rightarrow e^- + h^+ \tag{2}$$

$$e^- + O_2 \rightarrow O_2^- \tag{3}$$

$$h^+ + KMnO_4 \rightarrow degradation\ compounds \tag{4}$$

$$h^+ + H_2O \rightarrow OH^- + H^+ \tag{5}$$

$$OH^- + KMnO_4 \rightarrow degradation\ compounds \tag{6}$$

The adsorbed masses of $KMnO_4$ dye per unit mass of ZnO nanoparticles (q in mg/g) at any specific time and adsorption equilibrium were estimated using equations (7) and (8), respectively [29]:

$$q_t = (C_i - C_t)\frac{V}{W} \tag{7}$$

$$q_e = (C_i - C_e)\frac{V}{W} \tag{8}$$

, where q_t is $KMnO_4$ quantities adsorbed capacity at time (t), q_e is an equilibrium quantity adsorbed of $KMnO_4$, C_i is the initial concentration of $KMnO_4$ solution (mg/L), C_t is adsorbate concentrations (mg/L) at a time (t), C_e is an equilibrium adsorbate concentration (mg/L), V is adsorbate volume of $KMnO_4$ solution (L), and W adsorbent mass (g). Consequently, the dependence of adsorption capacity on the irradiation time is shown in Fig. 3. It was observed that

there is an improvement in the adsorption capacity as an increase in the irradiation time. The trend of the adsorption capacity is quite similar to the photocatalytic degradation efficiency curve as a function of the UV irradiation time. By other means, this trend confirms the increase of the computed photocatalytic efficiency presented in Fig. 2a and agrees with the previous studies [30, 31].
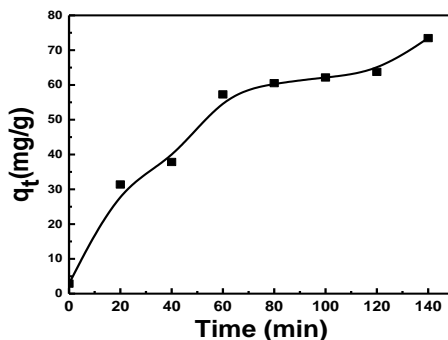

Fig. 3. Adsorption capacity (q_t) of KMnO$_4$ versus irradiation time on the ZnO nanoparticles.

In this section, three models are applied for analyzing the kinetics of the photocatalytic degradation experimental data called pseudo-first-order, pseudo-second-order, and intra-particle diffusion kinetic models and can be described by the following equations, respectively [32]:

$$\log(q_e - q_t) = log q_e - K_1 \frac{t}{2.303} \tag{9}$$

$$\frac{t}{q_t} = \frac{1}{K_2 q_e^2} + \frac{t}{q_e} \tag{10}$$

$$q_t = K_{diff}\sqrt{t} + C \tag{11}$$

, here K_1 and K_2 are the pseudo-first and pseudo-second-order constants (g/mg.min), respectively, $K_{diff.}$ is the intra-particle diffusion kinetic model (mg/g.min)$^{1/2}$, and C is a constant that provides an idea of the boundary-layer thickness [32].

The experimental data for the KMnO$_4$ adsorption kinetic onto the surface of ZnO nanoparticles were investigated by applying these previous models. The plots derived from equations 9-11 are shown in Figs. 4-6, respectively. The value of K_1, K_2, and K_{diff} was estimated and summarized in Table 1. These evaluated values as well as the values of q$_{max}$ and association coefficients (R^2) are summarized also in Table 1.

Table 1. Pseudo-first, pseudo-second-order parameters, and experimental q_e and parameter values of the intra-particle diffusion model for the $KMnO_4$ adsorption on ZnO nanoparticles.

Model	q_e exp. (mg/g)	73
Pseudo-first-order	q_e cal. (mg/g)	61.24
	q_e exp.- q_e cal	12.24
	K_1 (min^{-1})	1.7×10^{-2}
	R^2	0.94
Pseudo-second-order	q_e cal. (mg/g)	78.19
	q_e exp.- q_e cal	-5.19
	K_2 (g/mg·min)	5.7×10^{-4}
	R^2	0.93
Intra-particle diffusion	$K_{eff.}$ (mg/min$^{1/2}$g)	5.86
	C	4.47
	R^2	0.97

Fig. 4 shows the validity of applying the pseudo-first-order kinetic model for KMnO$_4$ adsorption on the ZnO nanoparticles. Fig. 4 shows a linear behavior between $\log(q_e - q_t)$ and t which is in agreement with Eq. 9, and accordingly the value of K_1 was estimated from the slope of the fitted line. The estimated value of K_1 was found to equal 1.7×10^{-2}, while the value of q_e equals 61.24 mg/g which is comrpared to the values in ref. [12] after modified equations. Similarly, Fig. 5 illustrates the validity of applying the pseudo-second-order kinetic model for KMnO$_4$ adsorption on the ZnO nanoparticles. The plotted data shows a linear plot corresponds to the relation of $\frac{t}{q_t}$ versus t. From the intercept of the fitted lines, the value of K$_2$ is obtained and equals 5.7×10^{-4} g/mg·min and is listed also in Table 1. It clears from Table 1 when applied the pseudo-second-order kinetic model to fit the obtained data R^2 equals 0.93 remarkably similar to that of the evaluated value (R^2~0.94) for the pseudo-first-order kinetic model. Furthermore, the values of q_e for KMnO$_4$ degradation using ZnO nanoparticles are estimated from the slope of the fitted line in Fig. 5 and listed in Table 1.
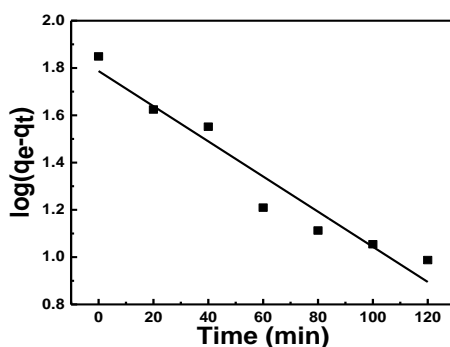

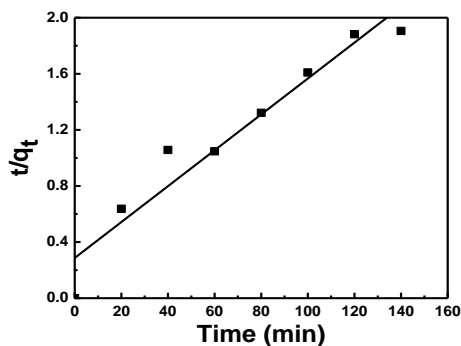*Fig. 4. Pseudo-first-order kinetic model for KMnO$_4$ adsorption on the ZnO nanoparticles.*

Fig. 5. Pseudo-second-order kinetic model for KMnO$_4$ adsorption on the ZnO nanoparticles.

The relation between q_t and $\sqrt{t}$, for the degradation process for KMnO4 dye using ZnO nanoparticles is shown in Fig. 6. From the obtained and fitted line, we have calculated both values of $K_{diff.}$ and C for ZnO nanoparticles. From the fitted line in this plot, the value of $R^2 > 0.97$. Therefore, these results indicate that the intra-particle diffusion kinetic model is the best model for describing the degradation mechanism for the adsorption of KMnO$_4$ dye onto ZnO nanoparticles compared to the first and second-order kinetic models. The estimated value of $K_{diff.}$ and C is 5.86 mg/min$^{1/2}$g, and 4.47, respectively, for adsorption of KMnO$_4$ dye onto ZnO nanoparticles. This designates that the adsorption of KMnO$_4$ dye on ZnO nanoparticles is conducted by a single step. The present deduced results are well matched with those reported in the literature [33].
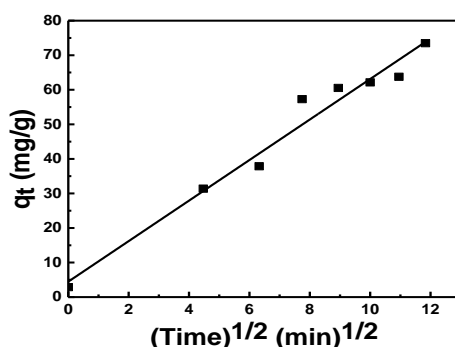

Fig. 6. Intra-particle diffusion model for KMnO$_4$ adsorption on ZnO nanoparticles.

To investigate the photocatalytic activity of ZnO nanoparticles, the degradation rate constants of KMnO$_4$ debasement were ascertained using the well-known Langmuir-Hinshelwood kinetics. The decomposition rate of the pseudo-first-order response is given from the following equation [34]:

$$\ln\left(\frac{c_t}{c_0}\right) = -kKt = -k_{app}t \tag{12}$$

, here k is the degradation rate constant, K is the adsorption equilibrium constant, and k_{app} is the apparent rate kinetic constant. Fig. 7 shows the plot of $\ln(C_t/C_o)$ versus the irradiation time (t). The relation is given by a straight line that well agrees with Eq. 12 and this confirms that the KMnO$_4$ waste is following the pseudo-first-order kinetics. The determined value of k_{app} was deduced from the slope of the fitted line and equals 5.5×10^{-2} /min.
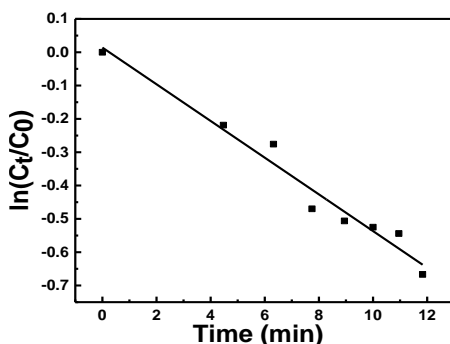
Fig. 7. Semi-logarithmic graph of KMnO₄ concentration versus irradiation time in the presence of ZnO nanoparticles.

Another equation that could be used for studying the photocatalytic degradation of the investigated sample is the Elovic equation. This equation is usually applied in the kinetics of the chemisorption of gases on solids. Besides, it can be used for investigating the adsorption of solutes from a liquid solution and written as following [35]:

$$q_t = \frac{\ln(\alpha\beta)+\ln(t)}{\beta} \tag{13}$$

, where α is the initial sorption rate (mg/g min), and β is a parameter that presents the extent of surface coverage and activation energy for chemisorption (g/mg). Fig. 8a shows the relation between q_t and $\ln(t)$ for the photocatalytic degradation of KMnO₄ dye in the presence of ZnO nanoparticles, which shows a linear curve for the plotted data and hence the well agree with Elovic kinetic model. The estimated value of α and β for the photocatalytic degradation of KMnO₄ dye in the presence of ZnO nanoparticles equals 42.6 mg/g min, and 4.7×10^{-2} g/mg, respectively.
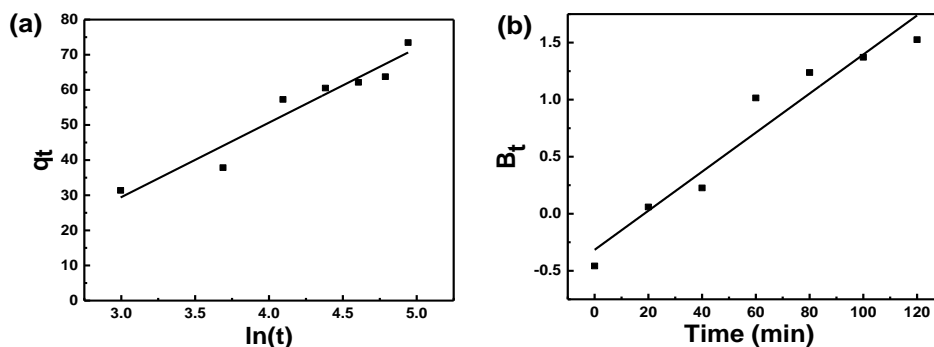

Fig. 8. Plots of (a) q_t versus ln(t), and (b) B_t versus the UV irradiation time (t) during the photocatalytic degradation of KMnO₄ in the presence of ZnO nanoparticles.

It is generally known, that the adsorption process is described through various steps such as (1) transport in solution bulk, (2) diffusion on the solid's surface, (3) adsorbate transport, and (4) sorption and desorption within the particle and solid's surface [36]. The processes (2), and (3) are called the rate-limiting processes while happening rapidly. Boyd et al. suggested [37] model be used for investigating the diffusion mechanism during the photocatalytic degradation process, and the equation written as following [37]:

$$B_t = -0.4977 - \ln(1 - \frac{q_t}{q_e}) \tag{14}$$

The above equation is a mathematical function of $(\frac{q_t}{q_e})$, and this ratio gives the fraction of adsorbate adsorbed at various irradiation time times. According to Boyd's model, the linear plot of B_t against t passes through the origin, which means the particle diffusion process is in control of the process; otherwise, the diffusion could be considered as the rate-limiting step of the process. The relation between B_t versus t presented in Fig. 8b and the plotted data gives a straight line, however, didn't pass through the origin which means the diffusion is classified as a rate-limiting step of the process.

4. Conclusion

In this study, ZnO nanoparticles were simply synthesized by the solid-solid reaction method. Their photocatalytic activity parameters, such as their efficiency and kinetic parameters on the $KMnO_4$ wasted water were tested and evaluated after 1 year from the synthesizing of ZnO. The photocatalytic efficiency values reached 47 % for ZnO nanoparticles, with these results suggesting ZnO nanoparticles' photocatalytic activity is higher for the removal of $KMnO_4$ dye over MB. Various models are applied to study the possible mechanisms through the photocatalytic degradation process. The greatest matching of the adsorption kinetic models has been observed for the intra-particle diffusion kinetic model compared to the pseudo-first-order, and pseudo-second-order models. Kinetics studies confirm that $KMnO_4$ adsorption onto ZnO nanoparticles is chemisorption.

Acknowledgment

References

[1] H. Rehman, Z. Ali, M. Hussain, S. R. Gilani, T. G. Shahzady, A. Zahra, S. Hussain, H. Hussain, I. Hussain, M. U. Farooq, Digest J. Nanomater. Biostruct. **14**(4), 1033 (2019).
[2] M. Fernández-García, A. Martínez-Arias, J. C. Hanson, J. A. Rodríguez, Chem. Rev. **104**, 4063 (2004).
[3] Al-Aoh, A. Hatem, Ibrahim A. M. Mihaina, Meshari A. Alsharif, A. A. A. Darwish, M. Rashad, Syed Khalid Mustafa, Meshari M. H. Aljohani, Mohammed A. Al-Duais, H. S. Al-Shehri, Chemical Engineering Communications, 1 (2019).
[4] Taha, A. Safeya, Alaa M. Abd-Elnaiem, Mansour Mohamed, Samar Mostafa, M. S. Mostafa, Desalination and Water Treatment **100**, 160 (2017).
[5] Arup Roy, Jayanta Bhattacharya, Nanotechnology in industrial wastewater treatment, IWA Publishing, 2015.
[6] Jacques C. Védrine, Catalysts **7**, 341 (2017).
[7] V. M. Samsonov, N. Yu Sdobnyakov, A. N. Bazulev, Surf. Sci. **526**, 532 (2003).
[8] M. Rashad, T. A. Hamdalla, S. E. A. Garni, A. A. A. Darwish, S. M. Seleim, Optical Materials **75**, 869 (2018).
[9] B. Tyagi, K. Sidhpuria, B. Shaik R. V. Jasra, Ind. Eng. Chem. Res. **4525**, 8643 (2006).
[10] M. Rashad, N. M. Shaalan, A. M. Abd-Elnaiem, Desalination and Water Treatment **57**(54), 26267 (2016).
[11] N. M. Shaalan, M. Rashad, M. A. Abdel-Rahim, Opt. Quant Electron **48**, 531 (2016).
[12] M. Rashad, Optical and Quantum Electronics **51**(9), 291 (2019).
[13] A. M. Smith, A. M. Mohs, S. M. Nie, Nat. Nanotechnol. **4**, 56 (2009).
[14] M. Fernandez-Garcia, X. Wang, C. B. Hanson, J. C. Iglesias-Juez, J. A. Rodriguez, Chem.

Mater. **17**, 4181 (2005).

[15] S. Surnev, G. Kresse, M. G. Ramsey, F. P. Netzer, Phys. Rev. Lett. **87**, 86102 (2001).

[16] M. Fernandez-Garcia, X. Wang, C. B. Hanson, J. C. Iglesias-Juez, J. A. Rodriguez, Chem. Mater. **17**, 4181 (2005).

[17] Jagriti Gupta, K. C. Barick, D. Bahadur, Journal of Alloys and Compounds **509**(23), 6725 (2011).

[18] Shuaishuai Ma, Rong Li, Changpeng Lv, Wei Xu, Xinglong Gou, Journal of Hazardous Materials **192**(2), 730 (2011).

[19] Teng Zhai, Shilei Xie, Yufeng Zhao, Xiaofeng Sun, Xihong Lu, Minghao Yu, Ming Xu, Fangming Xiao, Yexiang Tong, " Cryst. Eng. Comm. **14**(5), 1850 (2012).

[20] Jun Zheng, Zhi-Yuan Jiang, Qin Kuang, Zhao-Xiong Xie, Rong-Bin Huang, Lan-Sun Zheng. Journal of Solid State Chemistry **182**(1), 115 (2009).

[21] Raman Kr. Verma, Rishabh Kapoor, Shailendra Kr. Gupta, Rahul R.Chaudhari, Pharmaceutical and Chemical Journal **1**, 20 (2014).

[22] Guang-Xia Li, Yao-Hui Huaug, Teng-Chien Chen, Yu-Jen Shih, Hui Zhang, Appl. Sci. **2**, 166 (2012).

[23] H. Lin, W. Deng, T. Zhou, S. Ning, J. Long, X. Wang, Appl. Catal. B: Environ. **176-177**, 36 (2015).

[24] M. Rashad, Taymour A. Hamdalla, A. A. A. Darwish, S. M. Seleim, Mater. Res. Express, 6 (2019).

[25] H. Zhu, R. Jiang, Y. Fu, Y. Guan, J. Yao, L. Xiao, G. Zeng, Desalination **286**, 41 (2012).

[26] U. T. Nakate, Journal of Nanoparticles **2013**, 1 (2013).

[27] M. Curri, R. Comparelli, P. Cozzoli, G. Mascolo, A. Agostiano, Materials Science and Engineering C **23**, 285 (2003).

[28] Hatem. A. AL-Aoh, Desalination and Water Treatment **110**, 229 (2018).

[29] F. Ahmad, W. M. A. W. Daud, M. A. Ahmad, R. Radzi. Chem. Eng. J. **178**, 461 (2011).

[30] A. A. A. Darwish, M. Rashad, H. A. AL-Aoh, Dyes and Pigments **160**, 563 (2019).

[31] M. Rashad, H. A. AL-Aoh, Desalination and Water Treatment **139**, 360 (2019).

[32] F. Ahmad, W. M. A. W. Daud, M. A. Ahmad, R. Radzi. Chem. Eng. J. **178**, 461 (2011).

[33] Hatem. A. AL-Aoh, M. J. Maah, Rosiyah. Yahya, M. R. Bin Abas. Asian Journal of Chemistry **25**, 9582 (2013).

[34] Yan, Hongwei et al., Materials Research Bulletin **44**(10), 1954 (2009).

[35] Yasemin Bulut, Zeki Tez, Journal of Hazardous Materials **149**(1), 35 (2007).

[36] Gönül Akkaya, Ayla Özer, Process Biochemistry **40**(11), 3559 (2005).

[37] G. E. Boyd, A. W. Adamson, L. S. Myers Jr., " Journal of the American Chemical Society **69**(11), 2836 (1947).